HHS Public Access

Author manuscript

Chemistry. Author manuscript; available in PMC 2016 September 28.

Published in final edited form as:

Chemistry. 2015 September 28; 21(40): 13996–14001. doi:10.1002/chem.201502242.

Fluorogenic Strain-Promoted Alkyne-Diazo Cycloadditions

Dr. Frédéric Friscourt[a,b], **Prof. Dr. Christoph J. Fahrni**[c], and **Prof. Dr. Geert-Jan Boons**[a,*]

[a]Complex Carbohydrate Research Center, University of Georgia, 315 Riverbend Road, Athens, GA 30602, USA

[c]School of Chemistry and Biochemistry and Petit Institute for Bioengineering and Bioscience, Georgia Institute of Technology, 901 Atlantic Drive, Atlanta, GA 30332, USA

Abstract

Fluorogenic reactions in which non- or weakly-fluorescent reagents produce highly fluorescent products are attractive for detecting a broad range of compounds in the fields of bio-conjugation and material sciences. We report here that Fl-DIBO, a dibenzocyclooctyne derivative modified with a cyclopropenone moiety, can undergo fast strain-promoted cycloadditions under catalyst-free conditions with azides, nitrones, nitrile oxides as well as mono- and disubstituted diazo-derivatives. While the reaction with nitrile oxides, nitrones and disubstituted diazo compounds gave cycloadducts with low quantum yield, monosubstituted diazo reagents produced 1*H*-pyrazole derivatives that exhibited a ~160-fold fluorescence enhancement over Fl-DIBO combined with a greater than 10,000-fold increase in brightness. Concluding from quantum chemical calculations, fluorescence quenching of 3*H*-pyrazoles, which are formed by reaction with disubstituted diazo-derivatives, is likely due to the presence of energetically low-lying (n,π*) states. The fluorogenic probe Fl-DIBO was successfully employed for the labeling of diazo-tagged proteins without detectable background signal. Diazo-derivatives are emerging as attractive reporters for the labeling of biomolecules and the studies presented here demonstrate that Fl-DIBO can be employed for visualizing such biomolecules without the need for probe washout.

Keywords

click chemistry; cycloaddition; bioorthogonal; fluorogenic probe; cyclooctyne

Introduction

Over the past decade, bioorthogonal reactions have opened new avenues for the study of complex biomolecules in cells and organisms.[1] Proteins, lipids, and glycans have been successfully visualized by the selective incorporation of an abiotic chemical functionality (reporter) that can be reacted with a complementary bioorthogonal functional group linked to a diverse set of probes such as biotin and fluorescent tags.[2] A commonly employed

gjboons@ccrc.uga.edu, Fax: 706-542-4412.

[b]Dr. F. Friscourt, Current address: Institut Européen de Chimie et Biologie, Université de Bordeaux, INCIA, CNRS UMR 5287, 2 rue Robert Escarpit, 33607 Pessac, France

Supporting information for this article is available.

approach for incorporating a chemical reporter into biomolecules is by feeding a metabolic precursor functionalized with the reporter.[3] Alternatively, an exogenously administered enzyme and a corresponding activated biosynthetic substrate modified by the chemical reporter can be employed.[4] It has also been demonstrated that an artificial amino acid containing a reporter can be introduced into proteins by using genetic code expansion technology.[5] Bioorthogonal reactions have also found application in many other fields of research, and for example are commonly employed for the modification of polymers and nanoparticles for the development of smart material.[6]

Organic azides are the most versatile reporters due to their small size and virtual absence in biological systems.[7] They can be conjugated by Staudinger ligation using modified phosphines,[3b, 8] Cu(I)-catalyzed cycloaddition with terminal alkynes (CuAAC),[9] or by strain-promoted alkyne–azide cycloaddition (SPAAC).[10] The latter type of reaction, which employs strained alkynes such as difluorinated cyclooctyne (DIFO),[11] dibenzylcyclooctynol (DIBO),[12] and bicyclononyne (BCN),[13] is attractive because it is fast and does not require a potentially toxic metal catalyst. Other commonly employed bioorthogonal reactions include the inverse-electron demand Diels-Alder cycloaddition between alkenes and tetrazines.[14]

Bioorthogonal reactions in which non- or weakly-fluorescent reagents produce highly fluorescent products offer the possibility to greatly expand the detection of a broad range of compounds and are particularly advantageous for applications in which probe washout is not possible or desirable. A number of such fluorogenic probes have been developed based on CuAAC,[15] Staudinger ligation,[16] and inverse-electron demand Diels-Alder reactions.[17] All these probes were designed based on the concept of quenching established fluorophores such as anthracene,[18] BODIPY,[19] or coumarins[20] with a bioorthogonal moiety such as an azide or tetrazine. Upon reaction, the quenching functionality is converted to the corresponding cycloadduct and fluorophore emission is restored. While in principle the same approach could be used for strain-promoted cycloadditions, the corresponding tags would inevitably be much larger compared to the rather inconspicuous propargyl groups used in CuAAC, and the increased molecular size might adversely affect the properties of target molecules, especially with regard to their biodistribution and biological activity. For this reason, the preferred approach for developing a catalyst-free fluorogenic click reagent is to utilize azide as the tagging moiety and to integrate the cyclooctyne group into the fluorophore structure. A first attempt towards this goal was reported by Bertozzi and co-workers, who designed the fluorogenic reagent CoumBARAC by fusing the cyclooctyne ring with a coumarin fluorophore.[21] Although the reaction product with 2-azidoethanol exhibited a 10-fold increased emission compared to unreacted CoumBARAC, it exhibited a low fluorescence quantum yield and required excitation around 300 nm, a wavelength regime that is incompatible with many biological applications. Recently, we reported a dibenzocyclooctyne derivative (**1**, Fig. 1, Fl-DIBO), which upon reaction with an azide produces a cycloaddition product that is more than 1000-fold brighter compared to the unreacted reagent, offers a large Stokes shift, and can be excited above 350 nm, the typical cut-off wavelength of standard fluorescence microscopes.[22] Quantum chemical

calculations indicated that fluorescent activation was due to an enhancement in oscillator strength of the S_0–S_1 transition upon triazole formation.

We have demonstrated that in addition to azides, a number of other 1,3-dipoles, such as nitrones, nitrile oxides and diazo derivatives react readily with strained alkynes such as DIBO.[23] Various methods have been developed to incorporate these functional groups into biomolecules, and for example it was recently shown that a diazo derivative of *N*-acetylmannosamine endured cellular metabolism and could be incorporated into mammalian cell surface glycoproteins.[24] The chemoselectivity of diazo and alkynyl groups enabled dual labeling of cells and it was noted that the diazo group is approximately half the size of an azido group, thus providing unique opportunities for orthogonal labeling of cellular components. The favorable properties of nitrones, nitrile oxides, and diazo reagents prompted us to explore whether they could also be employed for fluorescence turn-on reactions with Fl-DIBO **1**.

Results and Discussion

Reaction of Fl-DIBO (1) with various 1,3-dipolar compounds

The previously reported Fl-DIBO probe **1** has the advantage of combining ease of preparation (5-step synthesis with 35% overall yield) with strong fluorescence enhancement upon reaction with azides such as benzyl azide **2** (Scheme 1A).[22] Intrigued by the Fl-DIBO turn-on properties, we hypothesized that strong fluorescence enhancements might be also achieved upon reaction with other 1,3-dipolar compounds such as nitrones, nitrile oxides, and diazo derivatives. Reaction of Fl-DIBO **1** with nitrone **3** and nitrile oxide **4** generated the corresponding cycloaddition products **6** and **7** in near quantitative yields (Scheme 1A). Both reactions were performed at room temperature in a mixture of dichloromethane and methanol (4:1, v/v) and were completed within two hours.

Although many diazoalkanes are too reactive to be isolated or used in a biological context, it is possible to stabilize these derivatives to attain compounds that can be employed for bioorthogonal reactions. To identify a diazo derivative that exhibits optimal properties, we explored the influence of substituents on the rate of reaction with **1** and on the photophysical properties of the corresponding cycloaddition products (Scheme 1B). Diazo derivatives **8a–c** and **9b** were prepared in good yield by MnO_2-mediated oxidation of the corresponding hydrazones (see Supporting Information), 9-Diazo-fluorene **8d** was synthesized from the corresponding azido-derivative following a reported protocol,[25] and diazoacetate **9a** was commercially available. While reaction of Fl-DIBO (**1**) with disubstituted diazo reagents **8a–d** produced the respective [3+2] cycloaddition products **10a–d**, the monosubstituted diazo reagents **9a** and **9b** yielded the thermodynamically more stable tautomers **11a** and **11b**, respectively (Scheme 1B). The structural assignments were based on chemical shift differences of the C3 ring carbon atom in the ^{13}C-NMR spectra. Consistent with formation of a 3*H*-pyrazole ring, all disubstituted diazo containing compounds produced cycloadducts with chemical shifts around 110 ppm (105.8 ppm for **10b**, 112.6 ppm for **10c** and 113.9 ppm for **10d**). In contrast, the cycloaddition products of the monosubstituted diazo reagents

produced substantially lower field resonances at 141.7 ppm (**11a**) and 144.3 ppm (**11b**), indicating the presence of a 1*H*-pyrazole ring.

The second-order rate constant for the cycloaddition reaction of Fl-DIBO (**1**) and commercially available diazo ester **9a** was determined by monitoring product formation by ^{1}H-NMR spectroscopy in a mixture of $CDCl_3$ and CD_3OD (Figure S9, Supporting Information). The measured second-order rate constant of 2.4×10^{-3} $M^{-1}s^{-1}$ was somewhat lower compared to the cycloaddition with benzyl azide **2** (1.9×10^{-2} $M^{-1}s^{-1}$).[22] The presence of the electron-withdrawing ethyl ester on the diazo reagent significantly stabilizes the HOMO of the 1,3-dipole, leading to a lower reactivity. Notably, diazo malonate **8a** showed no reactivity with Fl-DIBO (**1**). Nevertheless, the observed rate constant for the coupling with diazo ester **9a** still compares favorably with the reaction kinetics of the Staudinger ligation ($k = 1.5\times10^{-4}$ $M^{-1}s^{-1}$) or the cycloaddition reaction of the first-generation cyclooctyne ALO with benzyl azide ($k = 1.3\times10^{-3}$ $M^{-1}s^{-1}$).[10a]

Photophysical characterization

In order to evaluate the change in fluorescence brightness of the cycloaddition products compared to Fl-DIBO (**1**), we acquired absorption and emission spectra in methanol (Figure 1) and determined the respective fluorescence quantum yields with quinine sulfate as fluorescence standard ($\Phi_F = 0.54$ in 1.0 N aqueous sulfuric acid).[26] All pertinent photophysical data are compiled in Table 1. While the lowest energy absorption bands of all cycloadducts fall within a narrow range between 340–360 nm, the molar extinction coefficients differ by more than one order of magnitude, with isoxazole **7** and pyrazoles **11a–b** being the strongest absorbers. Compared to Fl-DIBO **1**, the fluorescence emission maxima of the cycloaddition products are significantly blue-shifted, and the observed quantum yields vary over a large range. For example, fluorescence emission of **6** containing the non-aromatic 2,3-dihydroisoxazole ring was effectively quenched, whereas isoxazole derivative **7** showed an 8-fold fluorescence enhancement over Fl-DIBO **1** and a red-shifted emission maximum compared to triazole **5** (514 nm *vs.* 489 nm). Whereas replacing the ester group in 1*H*-pyrazole **11a** with a phenyl substituent in **11b** yielded similar excitation and emission maxima along with a slightly improved quantum yield, the fluorescence emission of derivatives **10b–d** containing a disubstituted 3*H*-pyrazole ring was consistently quenched. It is also noteworthy that all cycloadducts **3, 5, 7** and **9** exhibit large Stokes shifts (>6000 cm^{-1}), making them less prone to self-absorption.

Altogether, the pyrazoles **11a** and **11b** displayed the strongest fluorescence increase with a quantum yield of around 30%. Combined with their large absorption cross section at an excitation wavelength of 370 nm, these cycloadducts are by more than 10,000-fold brighter compared to unreacted Fl-DIBO **1** (Table 1, last column), thus making monosubstituted diazo reagents potentially exciting chemical reporters as the photophysical properties of 1*H*-pyrazoles **11a** and **11b** are more favorable than those of cycoadducts of azides (**5**).

Computational studies

Intrigued by the strong fluorescence quenching of 3*H*-pyrazoles **10b–d**, we were interested in exploring potential differences in their excited state manifolds compared to the highly

emissive 1*H*-pyrazoles **11a** and **11b**. Of particular interest was the question to what extent energetically low-lying triplet $^3(n,\pi^*)$ states might contribute to fluorescence quenching in the 3*H*-pyrazole derivatives.[27] For this purpose, we utilized compounds **10b** and **11b** as representative model compounds and determined their vertical excitation energies based on TD-DFT quantum chemical calculations. Previous studies on Fl-DIBO **1** and triazole **5** showed that the long-range corrected hybrid functional CAM-B3LYP[28] with a polarized continuum model (PCM)[29] reproduced absorption and emission data quite well for this compound class. Following the same approach, we calculated the energies of the first four excited singlet states at the B3LYP/6–31+G(d)//B3LYP/6–31G(d) level of theory (Table 2) and analyzed the nature of each transition based on electron density difference plots (Figure 2). Consistent with the large molar extinction coefficient of 10,600 $M^{-1}cm^{-1}$ for the lowest-energy absorption band, the first excited singlet state S_1 of **11b** is dominated by a HOMO-LUMO transition with substantial oscillator strength. The corresponding electron density difference plot resembles the pattern previously reported for the lowest excited state of triazole **5**[22] indicating a symmetry-allowed π-π^* transition (Figure 2A). Although the closest higher-energy excited singlet state S_2 exhibits n-π^* character involving the carbonyl oxygen lone-pairs, there is a large energy separation of 0.74 eV between the two states such that the corresponding triplet $^3(n,\pi^*)$ state should remain above S_1 without interfering with radiative deactivation. The proposed energy ordering is supported by the inherently small singlet-triplet splitting of (n,π^*) states with $\Delta E_{ST} \sim 0.1$ eV.[30] In contrast, the lowest two excited states of 3*H*-pyrazole **10b** exhibit significant n-π^* character with involvement of the nitrogen lone pairs on the 3*H*-pyrazole ring (Figure 2B). Hence, the low fluorescence quantum yield of **10b** is likely caused by non-radiative deactivation through intersystem crossing to the corresponding triplet $^3(n,\pi^*)$ states. The presence of an energetically low-lying (n,π^*) state is further supported by the experimental absorption spectrum, which upon Gaussian fitting revealed a weak low-energy band with a small molar extinction coefficient around 800 $M^{-1}cm^{-1}$ (Figure 3). Furthermore, the intensity and position of the adjacent bands at shorter wavelengths fit qualitatively well with the oscillator strengths and transition energies predicted based on the TD-DFT calculations (Figure 3 and Table 2). Altogether, it can be concluded that the poor brightness of **10b** compared to **11b** is due to a much smaller absorption cross section combined with efficient fluorescence quenching, both of which are the result of energetically low-lying (n,π^*) states.

Protein labeling experiment

Next, we explored Fl-DIBO (**1**) as fluorogenic labeling agent for diazo-functionalized biomolecules. As diazo ester **9a** was found to be more stable than phenyl diazo methane **9b**, NHS-activated diazo ester **12**[31] was synthesized as amino-reactive reagent and employed to modify bovine serum albumin (BSA) as a model protein. The diazo ester **12** was attached to the protein surface using standard NHS-ester-coupling conditions (Figure 4A). Briefly, a solution of BSA (20 mg/mL) in PBS (pH 7.4) was incubated with a solution of NHS-activated diazo ester **12** (25 mM) in DMSO overnight at room temperature. The excess of low molecular weight NHS-activated diazo ester was removed by spin-filtration. Diazo-labeled BSA was then reacted with Fl-DIBO (**1**) at 37 °C for 18 hours and analyzed by in-gel fluorescence imaging. As depicted in Figure 3B, a strong fluorescent band (lane 3) was observed at 66 kDa, confirming the ligation reaction, while no reaction was observed in the

absence of either Fl-DIBO (lane 2) or diazo ester label (lane 4). As an additional control, diazo-conjugated BSA was exposed to DIBO-FITC[22] to yield a fluorescent band at 66 kDa (lane 5); however, faint labeling was also observed when DIBO-FITC was reacted with unmodified-BSA (lane 6). Cyclooctynes can react with thiol residues of proteins leading to background labeling.[32] Gratifyingly, Fl-DIBO did not exhibit fluorescence turn-on in the presence of unmodified BSA (lane 4).

Conclusion

We have explored fluorescence turn-on cyloadditions of Fl-DIBO **1** with a number of 1,3 dipoles including azides, nitrile oxides, nitrones, and diazo-derivatives. It has been found that reactions with nitrile oxides, nitrones, and disubstituted diazo derivatives give adducts in which the fluorescence emission is low or quenched. On the other hand, cycloadditions of Fl-DIBO **1** with monosubstituted diazo reagents give adducts that can tautomerise to aromatic 1*H*-pyrazoles (**11a** and **11b**) and exhibit a ~160-fold enhancement in fluorescence quantum yield combined with more than 10,000-fold increase in brightness. Photophysical properties of the pyrazoles, such as quantum yield, brightness and Stokes shift, are more favorable than those of triazoles formed by a cycloaddition with azides. Quantum chemical calculations have indicated that the poor brightness of **10b** compared to **11b** is due to a much smaller absorption cross section combined with efficient fluorescent quenching, both of which are the result of energetically low-lying (n,π*) states. The finding that the cycloadducts of Fl-DIBO with monosubstituted diazo-derivatives exhibit favorable fluorescent turn on properties, offers exciting opportunities for selective labeling of biomolecules in a complex biological environment.

Supplementary Material

Refer to Web version on PubMed Central for supplementary material.

Acknowledgments

This research was supported by the National Cancer Institute of the US National Institutes of Health (R01CA88986 to G-JB).

References

1. a) Patterson DM, Nazarova LA, Prescher JA. ACS Chem. Biol. 2014; 9:592–605. [PubMed: 24437719] b) Sletten EM, Bertozzi CR. Angew. Chem., Int. Ed. 2009; 48:6974–6998.c) Debets MF, Van Hest JCM, Rutjes FPJT. Org. Biomol. Chem. 2013; 11:6439–6455. [PubMed: 23969529]
2. a) Boyce M, Bertozzi CR. Nat. Methods. 2011; 8:638–642. [PubMed: 21799498] b) Hang HC, Wilson JP, Charron G. Acc. Chem. Res. 2011; 44:699–708. [PubMed: 21675729] c) Jing C, Cornish VW. Acc. Chem. Res. 2011; 44:784–792. [PubMed: 21879706]
3. a) Ngo JT, Champion JA, Mahdavi A, Tanrikulu IC, Beatty KE, Connor RE, Yoo TH, Dieterich DC, Schuman EM, Tirrell DA. Nat. Chem. Biol. 2009; 5:715–717. [PubMed: 19668194] b) Saxon E, Bertozzi CR. Science. 2000; 287:2007–2010. [PubMed: 10720325]
4. Mbua NE, Li X, Flanagan-Steet HR, Meng L, Aoki K, Moremen KW, Wolfert MA, Steet R, Boons GJ. Angew. Chem., Int. Ed. 2013; 52:13012–13015.
5. a) Lang K, Chin JW. Chem. Rev. 2014; 114:4764–4806. [PubMed: 24655057] b) Wan W, Huang Y, Wang Z, Russell WK, Pai PJ, Russell DH, Liu WR. Angew. Chem., Int. Ed. 2010; 49:3211–3214.

6. a) Canalle LA, Van Berkel SS, De Haan LT, Van Hest JCM. Adv. Funct. Mater. 2009; 19:3464–3470.b) Ledin PA, Kolishetti N, Boons GJ. Macromolecules. 2013; 46:7759–7768. [PubMed: 24511157]
7. Debets MF, van der Doelen CWJ, Rutjes FPJT, van Delft FL. ChemBioChem. 2010; 11:1168–1184. [PubMed: 20455238]
8. Schilling CI, Jung N, Biskup M, Schepers U, Bräse S. Chem. Soc. Rev. 2011:4840–4871. [PubMed: 21687844]
9. a) Meldal M, Tornoe CW. Chem. Rev. 2008; 108:2952–3015. [PubMed: 18698735] b) Kennedy DC, McKay CS, Legault MCB, Danielson DC, Blake JA, Pegoraro AF, Stolow A, Mester Z, Pezacki JP. J. Am. Chem. Soc. 2011; 133:17993–18001. [PubMed: 21970470] c) Soriano Del Amo D, Wang W, Jiang H, Besanceney C, Yan AC, Levy M, Liu Y, Marlow FL, Wu P. J. Am. Chem. Soc. 2010; 132:16893–16899. [PubMed: 21062072]
10. a) Debets MF, van Berkel SS, Dommerholt J, Dirks ATJ, Rutjes FPJT, van Delft FL. Acc. Chem. Res. 2011; 44:805–815. [PubMed: 21766804] b) Jewett JC, Bertozzi CR. Chem. Soc. Rev. 2010; 39:1272–1279. [PubMed: 20349533]
11. Codelli JA, Baskin JM, Agard NJ, Bertozzi CR. J. Am. Chem. Soc. 2008; 130:11486–11493. [PubMed: 18680289]
12. a) Friscourt F, Ledin PA, Mbua NE, Flanagan-Steet HR, Wolfert MA, Steet R, Boons GJ. J. Am. Chem. Soc. 2012; 134:5381–5389. [PubMed: 22376061] b) Ning X, Guo J, Wolfert MA, Boons GJ. Angew. Chem., Int. Ed. 2008; 47:2253–2255.
13. Dommerholt J, Schmidt S, Temming R, Hendriks LJA, Rutjes FPJT, Van Hest JCM, Lefeber DJ, Friedl P, Van Delft FL. Angew. Chem., Int. Ed. 2010; 49:9422–9425.
14. a) Devaraj NK, Weissleder R. Acc. Chem. Res. 2011; 44:816–827. [PubMed: 21627112] b) Kamber DN, Nazarova LA, Liang Y, Lopez SA, Patterson DM, Shih HW, Houk KN, Prescher JA. J. Am. Chem. Soc. 2013; 135:13680–13683. [PubMed: 24000889] c) Niederwieser A, Späte AK, Nguyen LD, Jüngst C, Reutter W, Wittmann V. Angew. Chem., Int. Ed. 2013; 52:4265–4268.
15. a) Le Droumaguet C, Wang C, Wang Q. Chem. Soc. Rev. 2010; 39:1233–1239. [PubMed: 20309483] b) Zhou Z, Fahrni CJ. J. Am. Chem. Soc. 2004; 126:8862–8863. [PubMed: 15264794]
16. Lemieux GA, De Graffenried CL, Bertozzi CR. J. Am. Chem. Soc. 2003; 125:4708–4709. [PubMed: 12696879]
17. a) Meimetis LG, Carlson JCT, Giedt RJ, Kohler RH, Weissleder R. Angew. Chem., Int. Ed. 2014; 53:7531–7534.b) Wu H, Yang J, Šečkute J, Devaraj NK. Angew. Chem., Int. Ed. 2014; 53:5805–5809.
18. Sawa M, Hsu T-L, Itoh T, Sugiyama M, Hanson SR, Vogt PK, Wong C-H. Proc. Natl. Acad. Sci. U. S. A. 2006; 103:12371–12376. [PubMed: 16895981]
19. Devaraj NK, Hilderbrand S, Upadhyay R, Mazitschek R, Weissleder R. Angew. Chem., Int. Ed. 2010; 49:2869–2872.
20. Sivakumar K, Xie F, Cash BM, Long S, Barnhill HN, Wang Q. Org. Lett. 2004; 6:4603–4606. [PubMed: 15548086]
21. Jewett JC, Bertozzi CR. Org. Lett. 2011; 13:5937–5939. [PubMed: 22029411]
22. Friscourt F, Fahrni CJ, Boons GJ. J. Am. Chem. Soc. 2012; 134:18809–18815. [PubMed: 23095037]
23. Sanders BC, Friscourt F, Ledin PA, Mbua NE, Arumugam S, Guo J, Boltje TJ, Popik VV, Boons GJ. J. Am. Chem. Soc. 2011; 133:949–957. [PubMed: 21182329]
24. Andersen KA, Aronoff MR, McGrath NA, Raines RT. J. Am. Chem. Soc. 2015; 137:2412–2415. [PubMed: 25658416]
25. Myers EL, Raines RT. Angew. Chem., Int. Ed. 2009; 48:2359–2363.
26. Demas JN, Crosby GA. J. Phys. Chem. 1971; 75:991–1024.
27. Lower SK, Elsayed MA. Chem. Rev. 1966; 66 199-&.
28. Yanai T, Tew DP, Handy NC. Chem. Phys. Lett. 2004; 393:51–57.
29. Tomasi J, Mennucci B, Cammi R. Chem. Rev. 2005; 105:2999–3093. [PubMed: 16092826]
30. Seixas de Melo J, Fernandes PF. J. Mol. Struct. 2001; 565–566:69–78.

31. Mukherjee M, Gupta AK, Lu Z, Zhang Y, Wulff WD. J. Org. Chem. 2010; 75:5643–5660. [PubMed: 20704436]

32. van Geel R, Pruijn GJM, van Delft FL, Boelens WC. Bioconjugate Chem. 2012; 23:392–398.

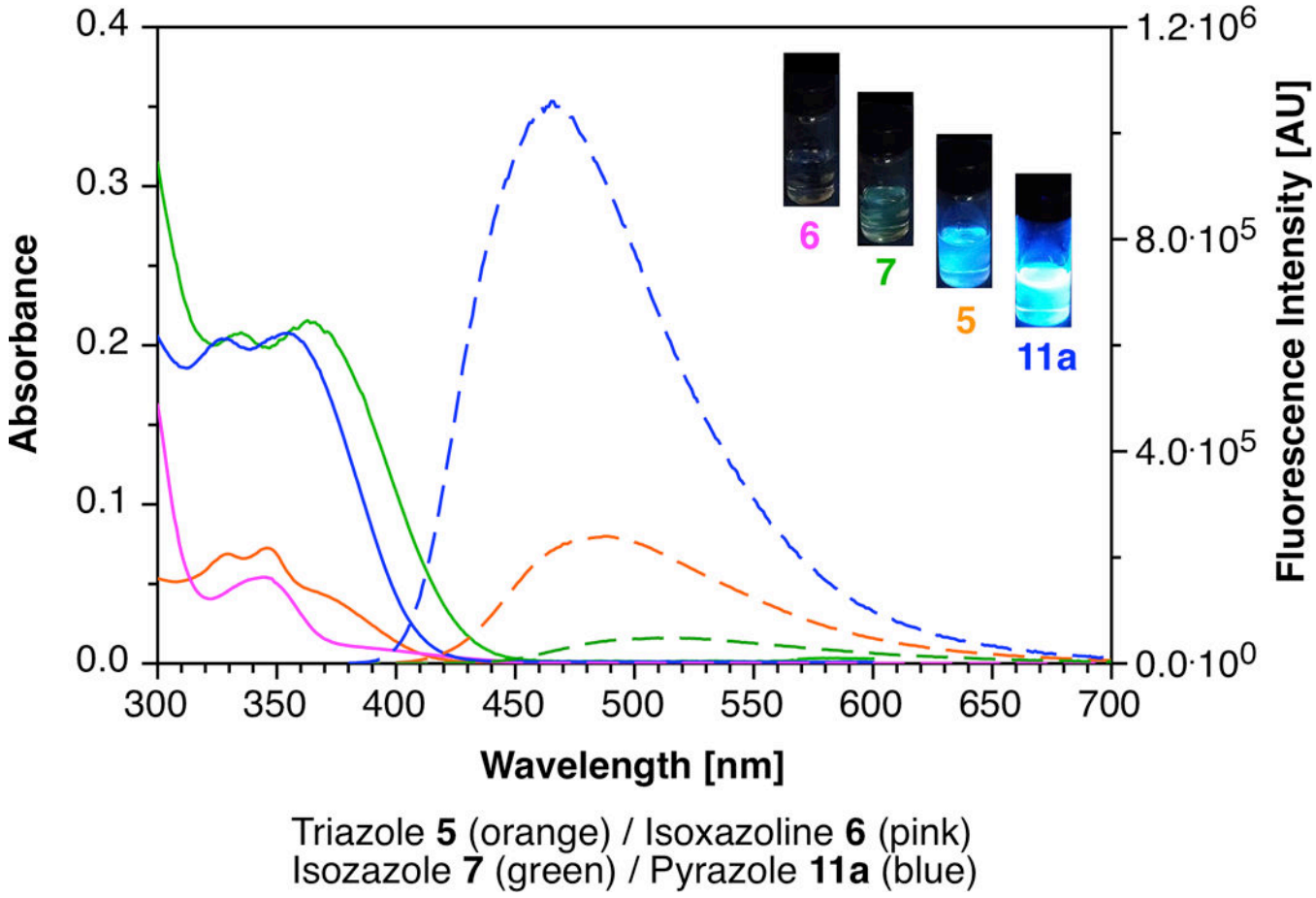

Figure 1.

Absorption (solid traces; 10 μM solutions) and fluorescence emission (dashed traces; λ_{exc} = 370 nm; OD_{370} = 0.75) spectra of cycloadducts **5, 6, 7** and **11a** in MeOH. Inset: Visual comparison of the fluorescence intensity of cycloadducts in MeOH with excitation at 365 nm.

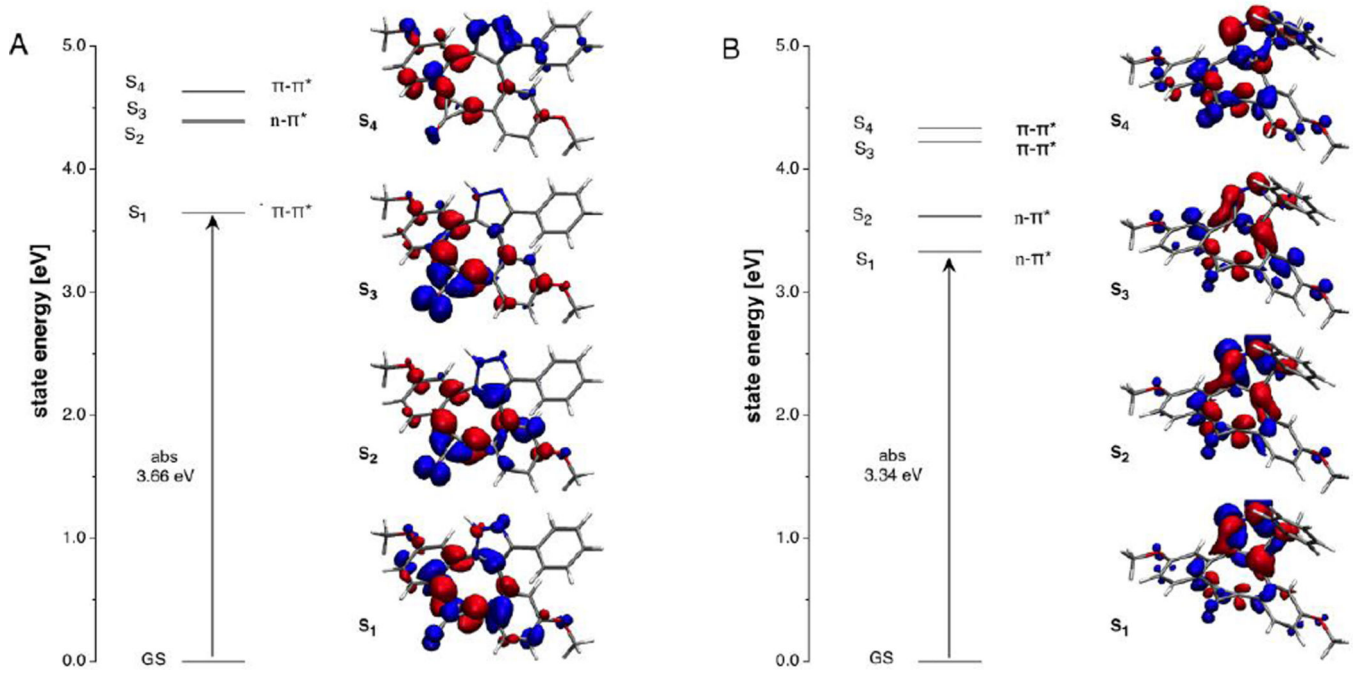

Figure 2.

Excited state manifold for (A) pyrazole derivative **11b** and (B) 3*H*-pyrazole derivative **10b**. The dual color plots illustrate the total electron density differences between each excited state and the corresponding ground state (decreasing intensity shown in blue, increasing density red; GS = ground state, S_1, S_2, S_3, and S_4 correspond to the four lowest-energy excited singlet states.

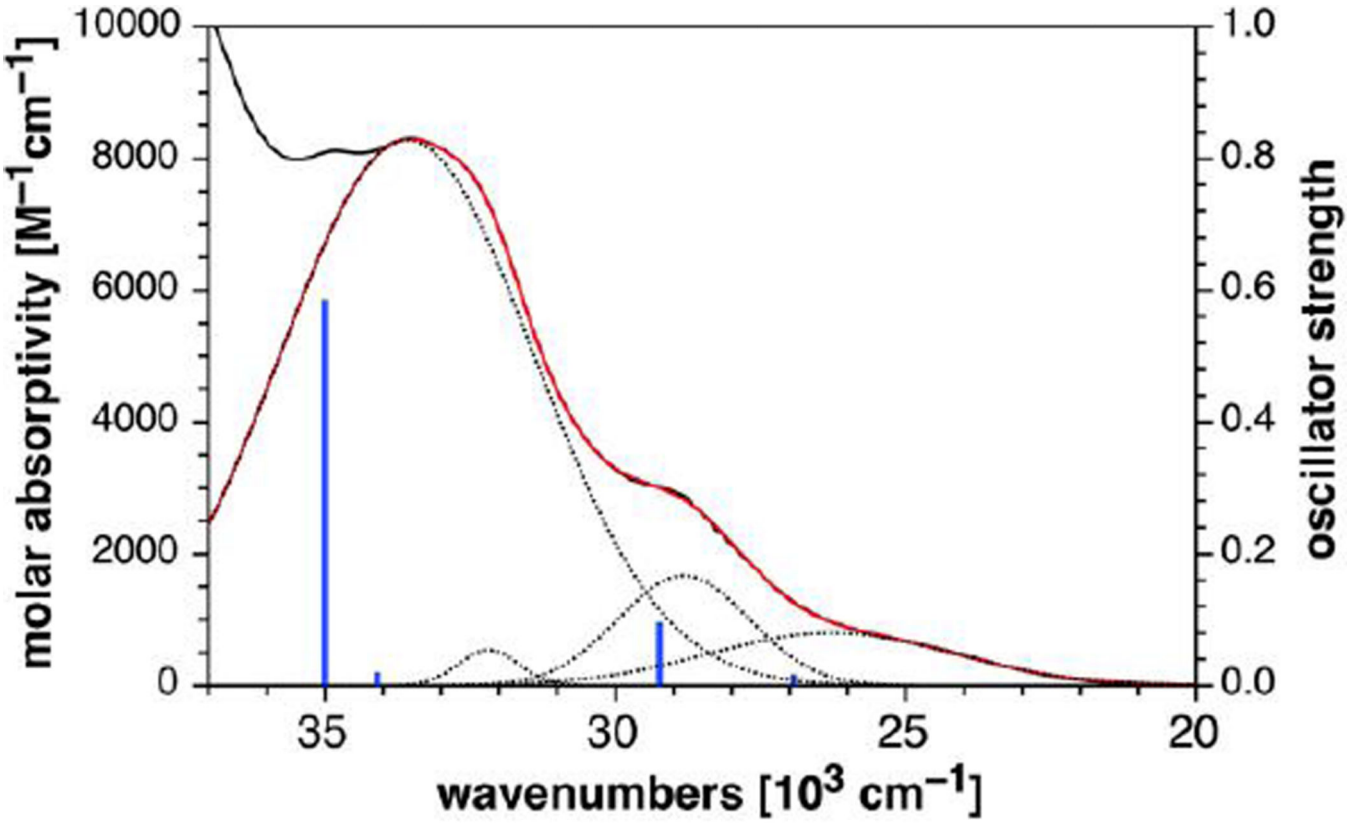

Figure 3.

Gaussian fitting (red trace) for the low-energy portion of the absorption spectrum (black trace) of 3*H*-pyrazole derivative **10b** and comparison to computed vertical excitation energies (blue lines) based on TD-DFT calculations (B3LYP/6–31+G(d)//B3LYP/6–31G(d) level of theory, PCM solvation with methanol). The dashed traces correspond to the individual bands extracted from a fit with four Gaussian functions. The experimental absorption spectrum is plotted on a molar absorptivity scale (left), whereas the intensities of the TD-DFT transitions are represented as oscillator strengths (right).

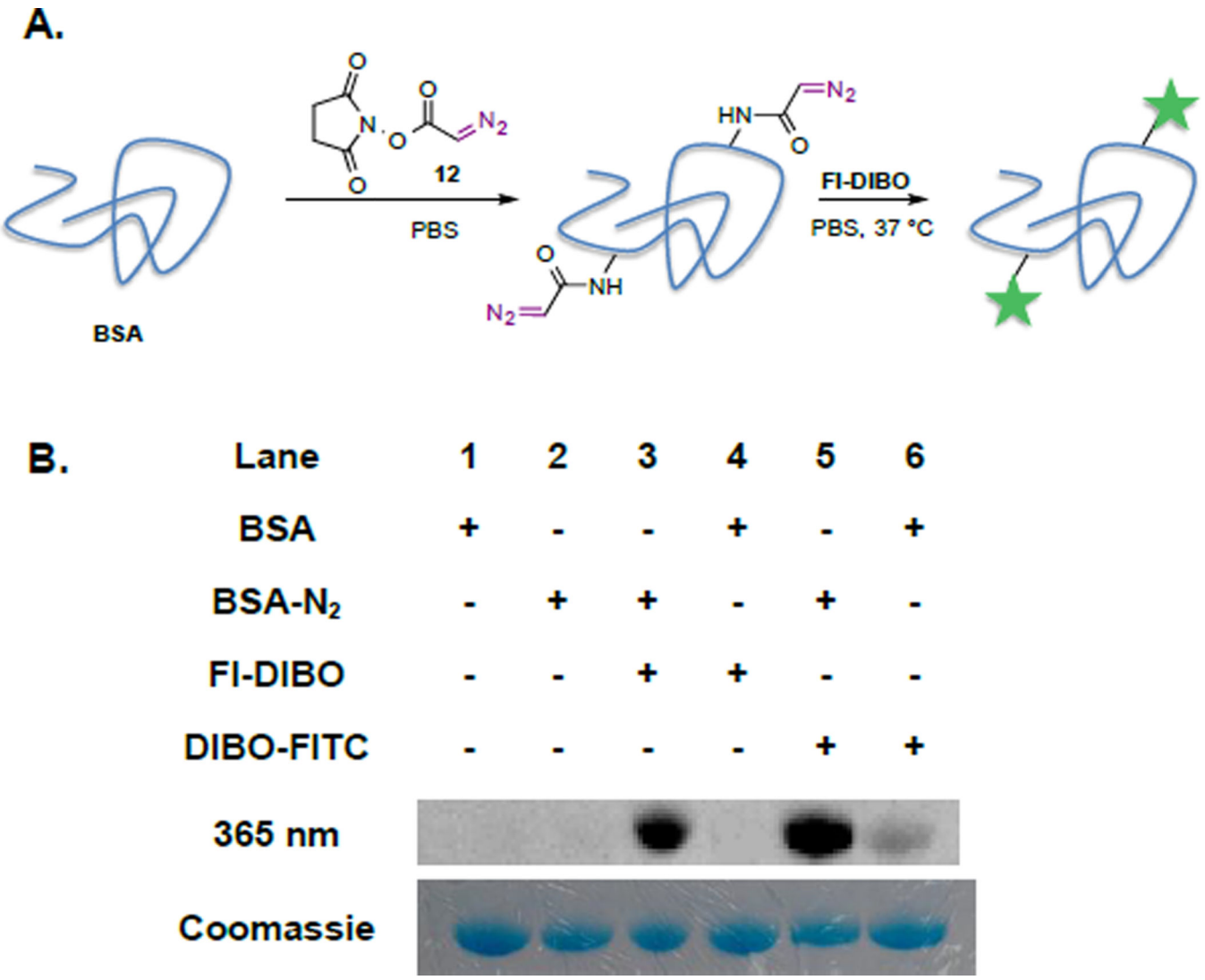

Figure 4.

Visualizing diazo-labeled proteins with Fl-DIBO (**1**) as fluorogenic reagent. **A.** Diazo-labeling of BSA (20 mg/mL in PBS) using NHS-activated ester **12** (25 mM in DMSO) and subsequent reaction with Fl-DIBO (**1**) (250 μM) overnight at 37 °C. **B.** In-gel visualization of labeled BSA with either Fl-DIBO or DIBO-FITC by fluorescence imaging (top row; $\lambda_{□□□}$ = 365 nm; λ_{detec} = 480 nm) and by Coomassie Blue stain to reveal total protein content (bottom row).

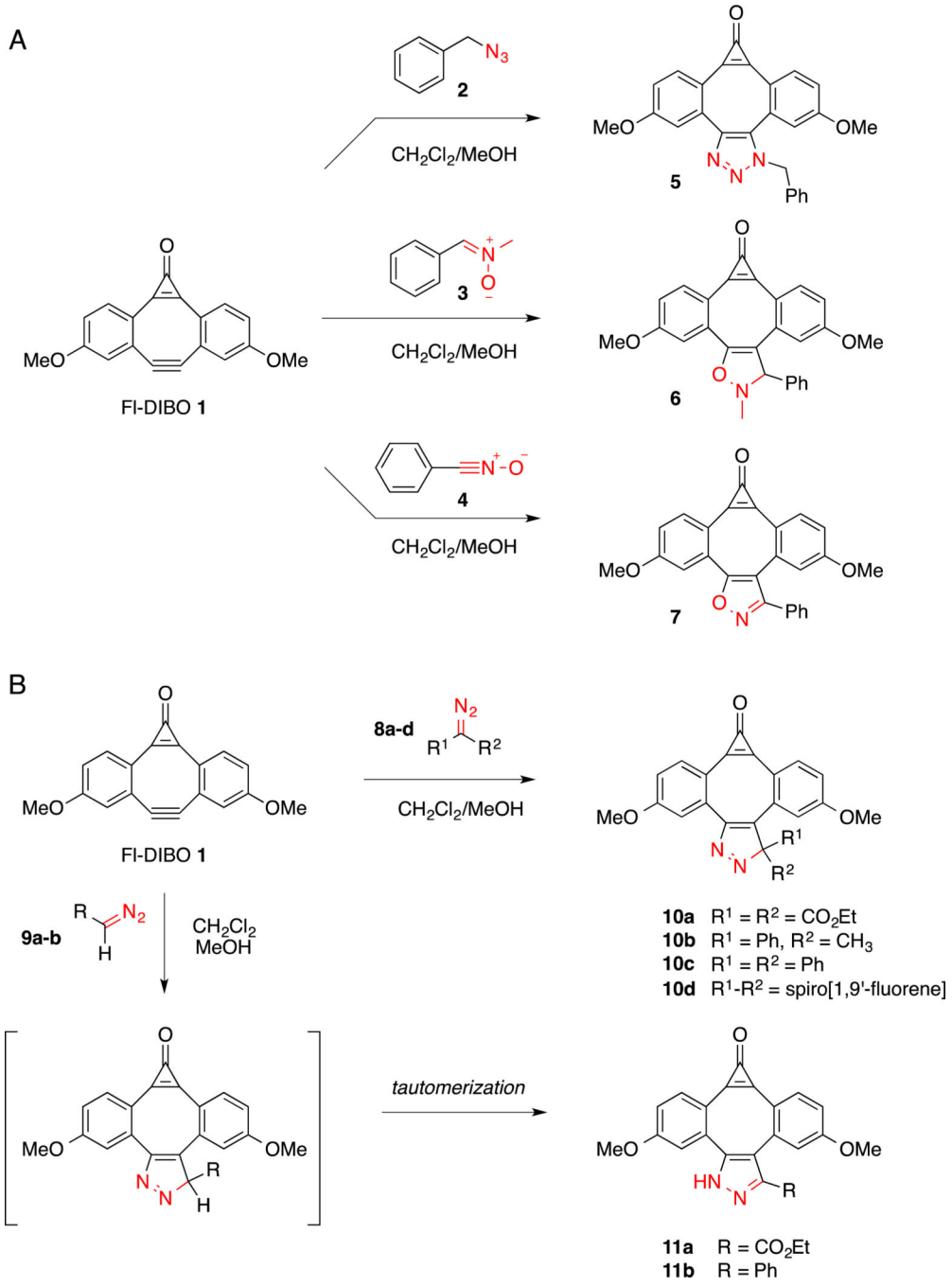

Scheme 1.
Reaction of Fl-DIBO with various 1,3-dipoles.

Table 1

Photophysical properties of Fl-DIBO **1** as well as cycloadducts **5–7, 10b–d**, and **11a–b** in MeOH at 298K.

Compound	λ_{abs} [nm]	ε_{abs} [$M^{-1}.cm^{-1}$]*a*	λ_{em} [nm]	Φ_F *b*	*c*	EF *d*
Fl-DIBO **1** *e*	420	150	574	0.002	0.3	1
5 *e*	364	4,600	489	0.12	550	1,800
6	345	1,330	-	<0.001	1	3
7	363	19,250	514	0.016	300	1,000
10b	350	1,300	n.d.	0.001	1	3
10c	361	3,000	n.d.	0.002	6	20
10d	370	2,100	n.d.	0.002	4	13
11a	360	13,400	463	0.30	4000	13,000
11b	370	10,600	469	0.32	3400	11,000

a Determined at 370 nm.

b Fluorescence quantum yield, quinine sulfate in 1.0 N H_2SO_4 as standard.

c Product of the extinction coefficient (at 370 nm) and the fluorescence quantum yield ($\varepsilon_{abs}\Phi_F$).

d Enhancement factor of the fluorophore brightness relative to Fl-DIBO **1**.

e Data from reference[22].

Table 2

Computational Data for Cycloaddition Products **10b** and **11b**.[a]

Compound	State	Energy TD-DFT [eV][b]	Oscillator Strength	Exp. Absorption [eV][c]	Exp. ε_{abs} [$M^{-1}cm^{-1}$][c]
10b	S_1 (n-π*)	3.34	0.013	3.26	800
	S_2 (n-π*)	3.63	0.091	3.57	1,700
	S_3 (π-π*)	4.23	0.016	3.99	540
	S_4 (π-π*)	4.34	0.581	4.16	8,300
11b	S_1 (π-π*)	3.66	0.205	3.42	10,600
	S_2 (n −π*)	4.40	0.086	n.d.	n.d.
	S_3 (n-π*)	4.42	0.068	n.d.	n.d.
	S_4 (π-π*)	4.65	0.025	n.d.	n.d.

[a] Calculated at the TD-CAM-B3LYP/6–31+G(d)//B3LYP/6–31G(d) level of theory.

[b] Vertical excitation energy

[c] Determined based on Gaussian fitting as illustrated in Figure 3.